

Biological applications of second harmonic imaging

Guy Cox

Received: 26 June 2011 / Accepted: 4 July 2011 / Published online: 20 July 2011
© International Union for Pure and Applied Biophysics (IUPAB) and Springer 2011

Abstract Second Harmonic Generation (SHG) microscopy dates back to 1974, but effective biological use of the technique has a history of barely 10 years. It is now widely used to image collagen in many different applications, and is becoming useful for imaging myosin and some polysaccharides. A separate line on research has focussed on SHG dyes, which can provide high-speed indication of membrane potential and are now in use in neurobiology. This review looks at the progress to date in these different fields.

Keywords Collagen · Myosin · SHG dyes · Polysaccharides · Second Harmonic Microscopy · SHG

Introduction

Some substances are able to generate the second harmonic—twice the frequency and half the wavelength—of an incident beam of light. This is a scattering process—no energy is lost—and it is a property exclusively of molecules with no center of symmetry. The electric field of the exciting light must be strong enough to modify the charge distribution in the molecule, which means that very intense light—typically a laser beam—is required. Second harmonic generation (SHG) was demonstrated almost as soon as lasers were available to excite it. In 1960, Theodore Maiman made to world's first laser—a flash-lamp pumped pulsed ruby laser operating in the far red at 697 nm. (It is still, incidentally, in working order and was recently demonstrated at a symposium to honor the 50th

anniversary of Maiman's achievement. To most subsequent laser users, such longevity would seem an impossible dream.) The next year, Franken et al. (1961) placed a quartz crystal in front of this laser and demonstrated that they could generate the second harmonic at 348 nm. Since then, many transparent crystals which generate the second harmonic more efficiently than quartz have been devised and these are widely used as frequency doublers for lasers. Solid-state green lasers, for example, are actually frequency-doubled near infrared lasers.

Hellwarth and Christensen (1974) were the first scientists to apply SHG to microscopy, by illuminating crystals of potassium deuterium hydrogen phosphate with focussed laser light in a conventional widefield microscope. Such an approach has little general application since, by illuminating the entire field at one time, the intensity is too low to generate significant harmonic signal from anything other than a very strong emitter. Scanning microscopy is a much more practical and useful approach, and was first demonstrated by Gannaway and Sheppard (1978). Even with the illumination focussed in just one spot, the continuous-wave laser used by Gannaway and Sheppard required samples which were strong harmonic generators, and the modern adoption of the technique has been enabled by the ready availability of pulsed lasers, which deliver very intense light in pulses of around 100 fs duration. The repetition rate is typically 80–100 Mhz, giving 10–12.5 ns between pulses. Averaged over time, the intensity is low enough not to harm the specimen, but within each pulse the intensity is enormous.

These lasers (typically titanium sapphire lasers, which are tuneable from ~600 nm to ~1,000 nm) are also used for multiphoton fluorescence microscopy (Denk et al. 1990), and SHG microscopy has a lot in common with multiphoton and is normally carried out on the same microscope

G. Cox (✉)
Australian Centre for Microscopy and Microanalysis,
University of Sydney,
NSW 2006, Australia
e-mail: Guy.Cox@sydney.edu.au

(and often at the same time). Both techniques are focal-plane selective without the need for confocal optics, and both offer a modest resolution improvement (since the point spread function is squared) over conventional microscopy at the same wavelength. Both also have the advantages of improved penetration and reduced damage conferred by the longer excitation wavelength. Since image formation takes place only in excitation (unlike confocal microscopy), chromatic aberration has no effect, and light can be collected with a widefield detector so that less signal is lost to scattering (Cox and Kable 2006).

There are also significant differences between the two imaging modes. Fluorescence always involves eventual damage to the fluorophore (bleaching), but in SHG energy is conserved and there is no damage associated with the imaging process. (Which is not to deny that too high a laser intensity can damage the sample.) SHG is a coherent process, so the signal is in phase with the excitation beam and at exactly twice the frequency. It is also essentially instantaneous. Fluorescence is incoherent, contains a range of wavelengths all longer than half the (two-photon) excitation wavelength, and is emitted over a period of nanoseconds (the fluorescence lifetime). The signals are therefore easy to distinguish. (There is the possibility of 3-photon excited fluorescence at the SH wavelength, but a narrow band-pass filter will effectively eliminate that.) A consequence of the coherent nature of SHG is that, if there are many molecules within the excitation spot, the signal will propagate most strongly in a forward direction (Cox and Kable 2006). There are exceptions to this as different molecular configurations can lead to different directions of propagation, and this can be exploited in characterization. Nevertheless, effective SHG microscopy will generally require a transmitted light detector, and this in turn will necessitate a high numerical aperture condenser for efficient signal collection.

Both fluorescence and harmonic microscopy can make use of intrinsic tissue components or applied dyes, but most fluorescence microscopy uses either introduced or genetically expressed fluorochromes, while most SHG microscopy to date has used intrinsic components.

Collagen

Collagen makes up about 6% of the mass of the vertebrate body, mainly in bone, cartilage, skin, interstitial tissues and basal laminae. It is the most important extracellular structural protein of the animal body. Polymerized collagen forms a triple-helix from three of the primary alpha chains (Lodish et al. 2000). Multiple forms of collagen, with minor differences in minor amino acid composition, are coded separately in the genome. They have different conforma-

tions and fulfil different functions. Types I, II, III and V form fibrils, type IV forms sheets in basal laminae, and types VI and IX act as linkers, binding fibrillar collagen to other cell components. Type I, in particular, is highly crystalline, and is an important structural component of bone, cartilage and soft tissue. This makes it particularly effective for SHG, a fact which has been known for many years (Roth and Freund 1981; Freund et al. 1986). Harmonic generation is more or less independent of wavelength over a wide range (Georgiou et al. 2000), so that the laser wavelength can be chosen to suit other experimental needs. Early work made use of custom experimental optical systems which were not suitable for high-resolution imaging, and diffraction-limited SHG microscopy of collagen has a history of no more than 10 years (Campagnola et al. 2002; Cox et al. 2003; Zipfel et al. 2003).

In tissues, type I collagen gives a much stronger SH signal than other forms. In Fig. 1, we can see that the allografted kangaroo tail tendon (Type I) gives a strong and clear SH signal while the surrounding mouse Type III collagen gives no visible signal at these instrument settings. This provides a distinction between the two types which the Sirius Red staining of this slide does not give (Cox et al. 2003). Prima facie, this can be explained by the much higher crystallinity of type I collagen in the body, and Xu et

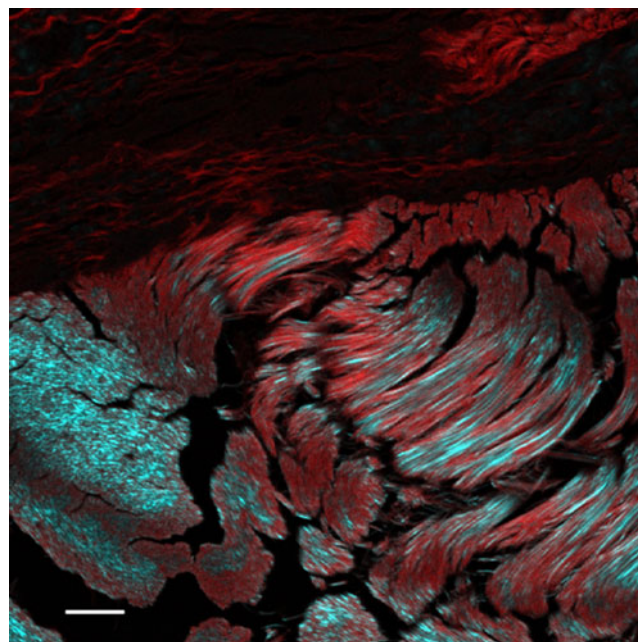


Fig. 1 Kangaroo tail tendon allografted into mouse tissue. The sample has been stained with Sirius red, which gives the red signal by two-photon fluorescence. The type I collagen of the kangaroo tendon (*bottom*) shows a strong SH signal (*cyan*). Type III collagen from the mouse (*above*) stains strongly with the Sirius red but shows little SH signal at this setting. *Scale bar* 25 μm . Sample courtesy Allan Jones. See Cox et al. (2003)

al. (2004) showed that in amorphous form the three major collagens types (I, II and III) gave identical SH signals. Amorphous collagen also gave signal propagation in both forward and backward directions, whereas crystalline collagen showed a strong tendency for forward propagation. Crystallinity also affects the polarization properties. Amorphous collagen of both types I and II gave a second-harmonic signal which was preferentially polarized at right-angles to the exciting beam. However, when these were gradually polymerized into fibrillar collagen under the microscope, type II retained the same polarization, whereas type I shifted the plane of polarization to be parallel to the exciting beam (Xu et al. 2004). Both direction of polarization and direction of propagation therefore seem to have promise as analytical tools in biology (Williams et al. 2004). Xu et al. (2010) recently refined this into a detailed structural analysis of collagen microstructure. However, to date most biologists have not made use of these tools, focussing instead on the exquisite sensitivity of SHG imaging to reveal collagen organization and remodeling in tissue under normal and pathologic conditions.

Liver fibrosis

Fibrosis (cirrhosis) of the liver is characterized by invasion of liver parenchyma by collagen fibres, and may result from chemical poisoning, hepatitis or genetic factors. Fibrosis is mediated by the activation of stellate cells in the parenchyma to express fibroblast activation protein (FAP), and the consequential deposition of collagen fibrils which eventually form dense septa. The collagen deposition can be viewed with exquisite sensitivity using SH imaging, and is visible and quantifiable at a much earlier stage than by conventional histological methods. The expression of FAP can be imaged simultaneously by one or two photon fluorescence (Cox et al. 2002; Gorrell et al. 2003), (Fig. 2).

Sensitive and accurate quantitative assays of the degree and progress of fibrosis have been developed using SHG imaging (Tai et al. 2009; Gailhouste et al. 2010). These are much more precise than techniques based on staining, and are totally objective rather than relying on the judgment of a clinician. The Fibro-C Index technology devised by Dean Tai, in Hanry Yu's laboratory, has now been spun off into a commercial start-up company, Histoindex Pte (<http://www.histoindex.com/>)

Normal structure and development

The combination of sensitivity, depth penetration, and 3D imaging has enabled novel insights in collagen deployment in many tissues. Manconi et al. (2001) used the technique as part a long-running study into structure and developmental changes in the human endometrium, a topic of great

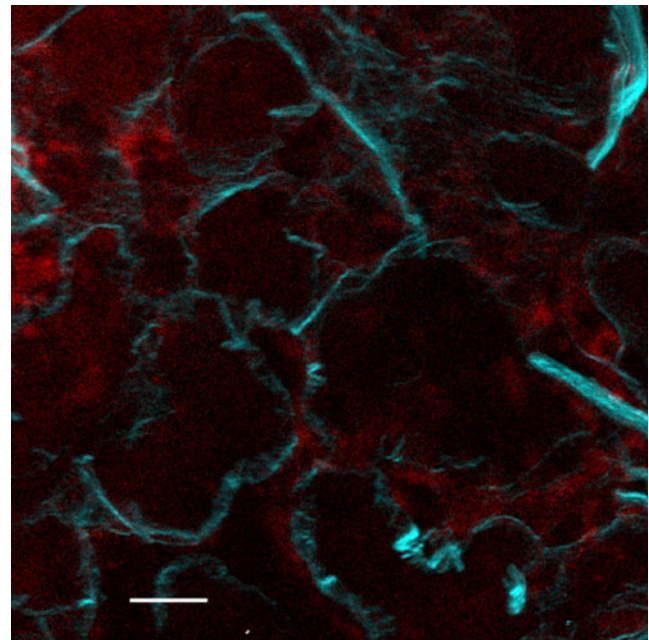


Fig. 2 Early stages of collagen deposition in liver parenchyma. Cyan is SH signal from collagen, red is single-photon fluorescence of CY5 labeled FAP. Scale bar 20 μm . See Cox et al. (2003) and Gorrell et al. (2003)

importance in fertility research (Fig. 3). An added bonus is that this tissue is strongly autofluorescent, so having a signal which is detectable without any interference from fluorescence is extremely useful.

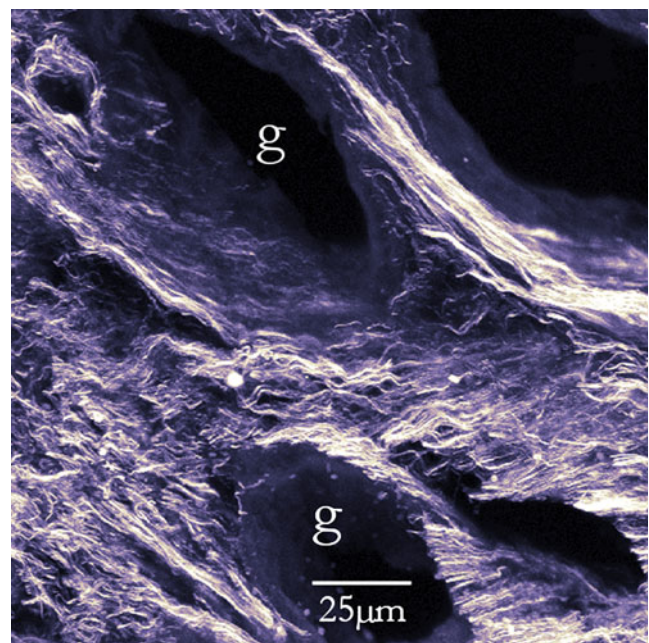


Fig. 3 SH image of collagen in human endometrium. 15° angle 3D projection from sections through an unfixed 15 μm cryosection. The pits (g) are where mucus glands are situated. From Cox et al. (2003), see also Manconi et al. (2003)

Tooth structure has also been investigated (Chen et al. 2007). The enamel showed strong two-photon autofluorescence enabling the structure of the rods to be seen, while the collagen gave a strong SH signal (Fig. 4.)

Collagen remodelling in cancer

Many cancers are characterized by remodeling of collagen fibres, and second harmonic imaging has become the tool of choice for investigating this. Typically collagen increases in amount as well as showing altered fibril orientation in malignant tissue. This has been shown in many different tumour types: breast cancer (Provenzano et al. 2008), ovarian cancer (Nadiarnykh et al. 2010) and melanoma (König and Riemann 2003).

The extent of collagen remodelling in ovarian cancer is illustrated in Fig. 5, from Nadiarnykh et al. (2010). These authors used a variety of quantitative techniques, including the ratio of forward to backward propagation of signal, spectral differences, and signal polarization, and were able to demonstrate clear and reproducible differences between tumours and normal tissue. The only commercial exploitation of this approach, to date, is the JenLab Derma-Inspect (König and Riemann 2003) which is used for in-vivo imaging of a patient's skin, using both multiphoton-excited fluorescence and SHG (in backscattered mode only, of course), and is used in diagnosis of melanoma and other skin conditions.

A note of caution is struck by a paper from Raja et al. (2010). They used a pulse-modulated SHG microscope,

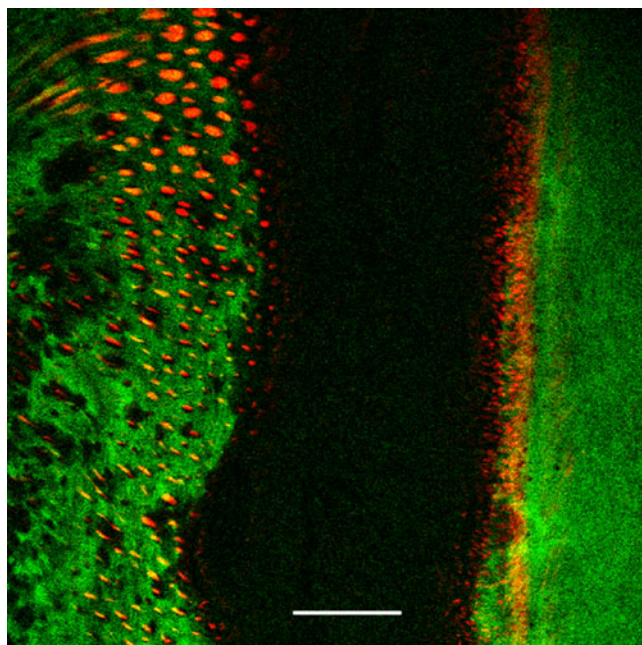


Fig. 4 The enamel region just beneath the gum in a developing tooth; single optical section. *Green* fluorescence from Masson's trichrome histological stain; *red* SH signal from collagen. *Scale bar* 100 μm . Sample courtesy Ann Swan. See Cox et al. (2002)

which they report gives improved signal to noise with weak collagen signals, to image collagen distribution in human acute myeloid leukemia. One of their findings was that, in patients treated with a new chemo-therapeutic agent targeting tyrosine kinase, the amount of collagen actually increased. Since the collagen scaffold is widely interpreted as facilitating cancer cell proliferation, it would suggest that collagen distribution should be tested when evaluating new drugs for chemotherapy.

Tendon damage

Injury to tendons, both acute and chronic, is a major concern in sports medicine. It is equally a concern, for the same reasons, in the horse-racing industry. Fung et al. (2010) studied isolated mouse tendons subjected to low, moderate and high fatigue loadings. At low loadings, kinking of collagen was observed, followed by fiber dissociation at moderate levels. At high levels, fibers thinned or became dissociated.

Sivaguru et al. (2010) studied tendon injury induced in a living horse by injection of collagenase into the superficial digital flexor (SDF) tendon of a living horse, using the corresponding tendon on the other limb as a control. Metrics included fiber orientation measured by Fourier transform, and ratio of forward to backward propagation, and again injury was accompanied by increasing disorientation of the fibrils. This study, like that of Fung et al., involved killing the animal, which is clearly not a very useful method for either a human athlete or a racehorse. Figure 6, which derives from unpublished work by Regina Cramer and the author, shows that it is, in principle, quite possible to work with biopsies from living subjects, and this is likely to be focus of future research

Myosin

Mouse muscle was shown to give a strong SH signal by Mohler et al. (2003). This was able to give high-resolution images even at considerable penetration distances. To establish the source of the signal, they turned to a simpler organism, the nematode *Caenorhabditis elegans*, and were able to demonstrate, using GFP-myosin constructs and mutant strains, that at least the bulk of the signal came from myosin heavy-chain B. This provided a useful tool for studying myosin arrangement in normal and diseased muscle.

Ralston et al. (2008) used the combination of SH myosin imaging and 2-photon fluorescence to investigate muscle damage in Pompe disease, which is a hereditary disease caused by mutations in the enzyme acid α -glucosidase. Using both mouse models (Fig. 7) and human biopsy

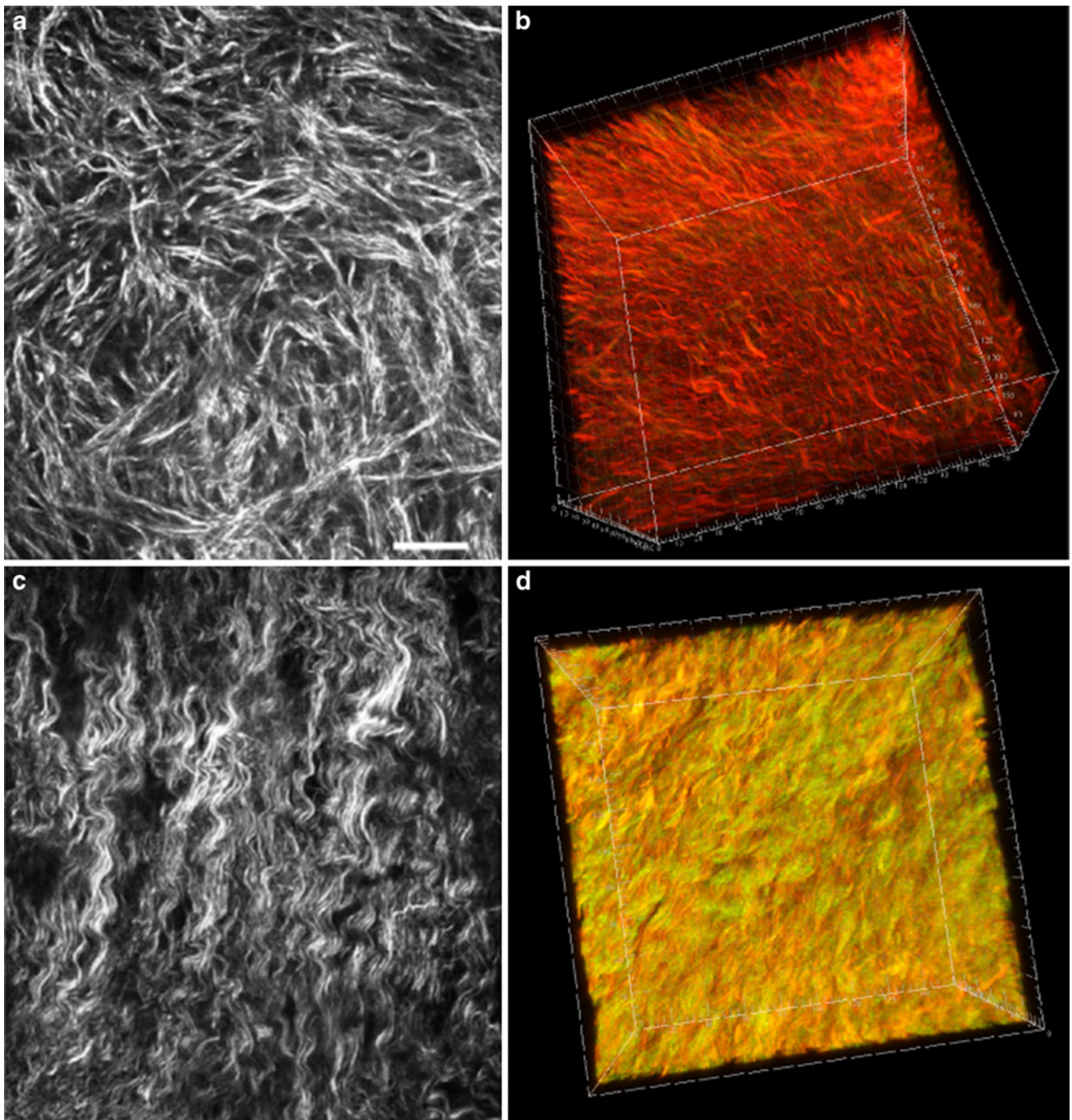


Fig. 5 Collagen remodeling in ovarian cancer, from Nadiarnykh et al. 2010. **a, b** Normal tissue, **c, d** tumour; **a, c** single optical sections, **b, d** 3D reconstructions. Scale bar 25 μm

material, they were able to demonstrate significant muscle disruption from accumulations of autophagic debris, as well as the enlarged lysosomes typical of the disease. Wallace et al. (2008) used 2-photon fluorescence to measure the volume of isolated fetal cardiomyocytes and the SH signal to measure the volume of myosin, from which they were able to calculate the myosin content of each cell. They

propose to make use of this technique to study developmental abnormalities in the fetal heart.

A recent paper by Nucciotti et al. (2010) was able to demonstrate, by SHG, changes in myosin conformation representing the action of the muscle motor, illustrating that the technique is now able to give fundamental insights into muscle function. Another recent paper, Brüggemann et al.

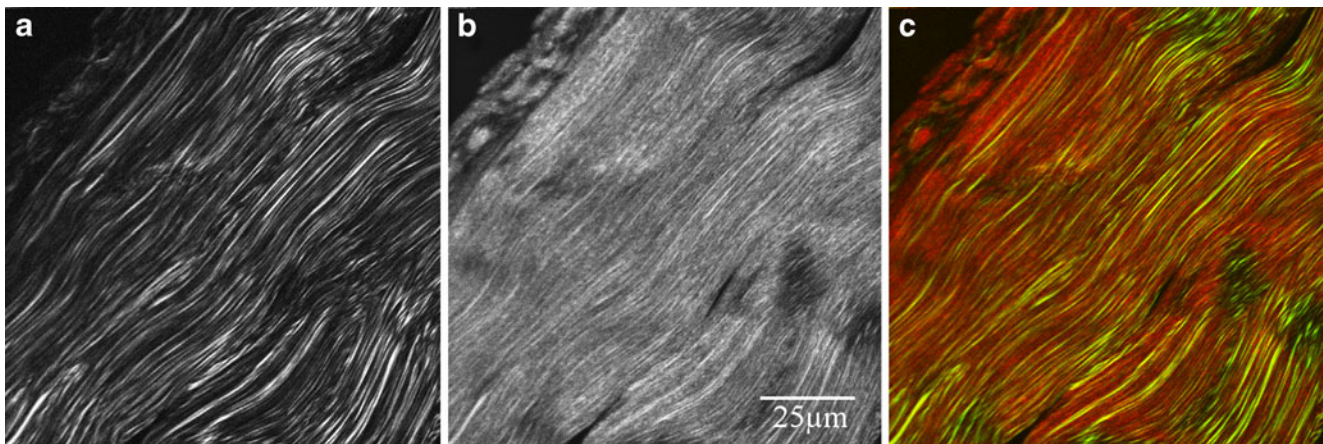


Fig. 6 Human Achilles tendon biopsy, from a fit and healthy athlete. (Sample provided by Regina Crameri). **a** Forward propagated SH signal, **b** back-propagated SH signal, **c** the two signals merged. From Moreno et al. (2004)

(2010) put the technique to a different use, namely the detection of thermally-induced changes in meat (in simpler terms, cooking). They found that the myosin signal from pork vanished at 53°C, whereas that of collagen persisted until ~60°C. This gives a high-tech demonstration that it takes a lot more cooking to make gristle tender than is needed for meat, which is not a surprising conclusion.

Polysaccharides

Both cellulose and starch are capable of giving SH signals. Both are highly significant polysaccharides:

cellulose is the essential structural component of plant cell walls, while starch is the commonest plant storage polysaccharide, and a major component of many food-stuffs. Cellulose is a β 1:4 linked glucan; alternate glucose residues are in reversed orientations which gives a certain amount of symmetry to the molecule, though the chirality of the glucose means that the symmetry is not complete. It is, therefore, a rather weak SH generator, even though it is highly crystalline. Starch, on the other hand, is α 1:4 linked, so each glucose molecule in the chain is in the same orientation, making the chain much less symmetrical. It gives a very strong SH signal, particularly when in a highly crystalline form.

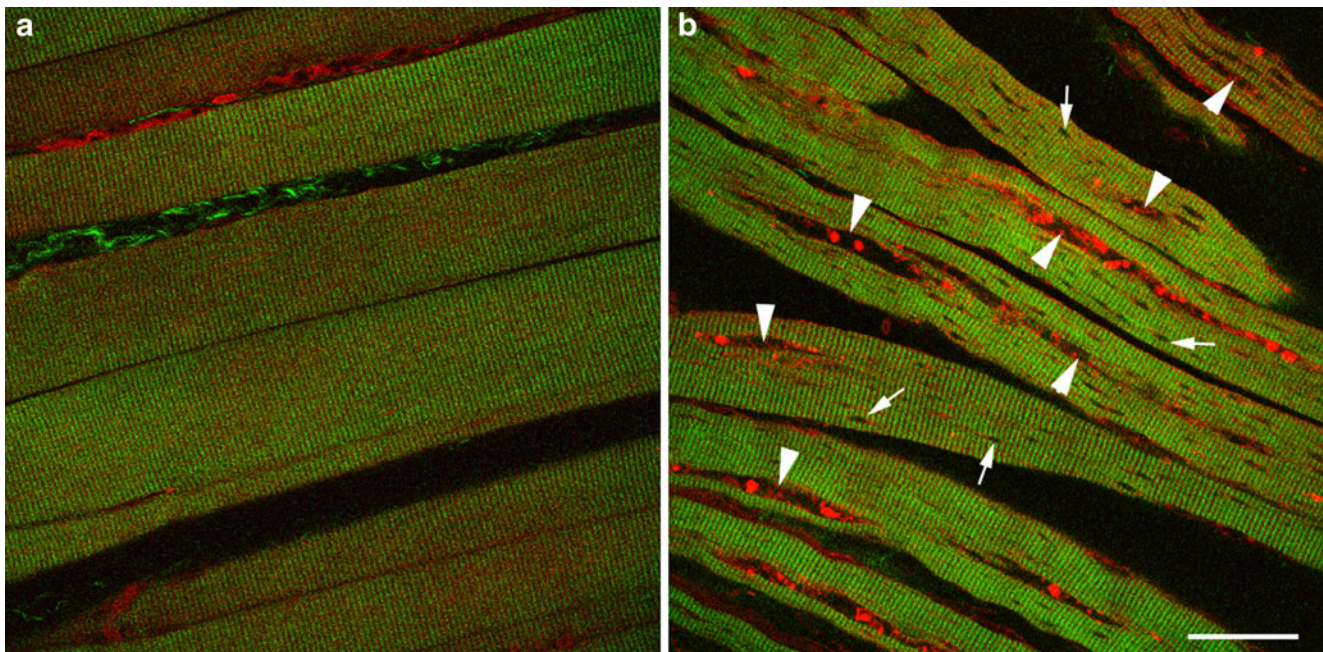


Fig. 7 Muscle disruption caused by mutations in acid α -glucosidase: **a** normal, **b** defective (GAA knockout). *Green* SHG, *red* 2PEF. *Arrowheads* show accumulations of autophagic debris, *small arrows* show the enlarged lysosomes. *Scale bar* 40 μ m. From Ralston et al. (2008)

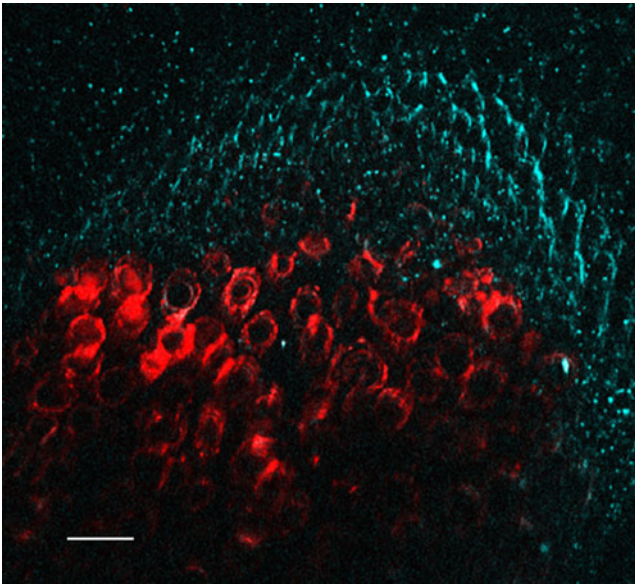


Fig. 8 Low-power image of vascular bundle in celery (*Apium graveolens*). Cyan is the SH signal, showing starch grains (dots) and cellulose (network). Red is the 2-photon signal from lignin autofluorescence. Scale bar 50 μm . See Cox et al. (2005)

Starch was first studied by SHG in 2000 (Mizutani et al. 2000). As with early studies of collagen, the setup was rather different to that used later since a widefield microscope illuminated with a pulsed neodymium laser was used. This is not depth selective and hence negates one of the main advantages of the technique. The following year, Chu et al. (2001) imaged plant cells with the more

conventional scanning technique, using a chromium forsterite laser at 1,250 nm. They were able to image both cellulose and starch, but neither of these pioneering papers achieved high resolution.

The first high-resolution study was that of Cox et al. (2005) using regular Ti-S lasers at 800–850 nm wavelengths. They looked at a wide range of samples: plant tissues, isolated starch grains and foodstuffs. Figure 8 shows a portion of celery petiole. The bundle-cap, made up of thick-walled collenchyma cells, gives a very visible cellulose SH signal, while the thin-walled parenchyma cells around it show only a faint signal from the wall, but numerous small starch grains. The tracheids of the xylem show strong lignin autofluorescence from their spirally-thickened walls.

There are two common forms of starch, amylose, which has only α 1:4 linked glucose with typically long chain lengths, and amylopectin which has branches introduced by α 1:6 linkages, and typically shorter chains. The polarization dependence of the SH signal from starch (Fig. 9) was studied in great detail by Zhou et al. (2010). They came to the conclusion that amylopectin was the major SH generator, and were able to determine molecular orientations with great precision.

Processing of starchy foods for consumption is fundamentally breaking down crystalline starch into an amorphous form which is more hydrophilic, more digestible and more palatable. This is what makes a cooked potato soft, for example. Subsequent recrystallization (retrogradation) causes defects in products such as lumpiness in sauces and staling of bread. Preventing this to extend shelf-life and

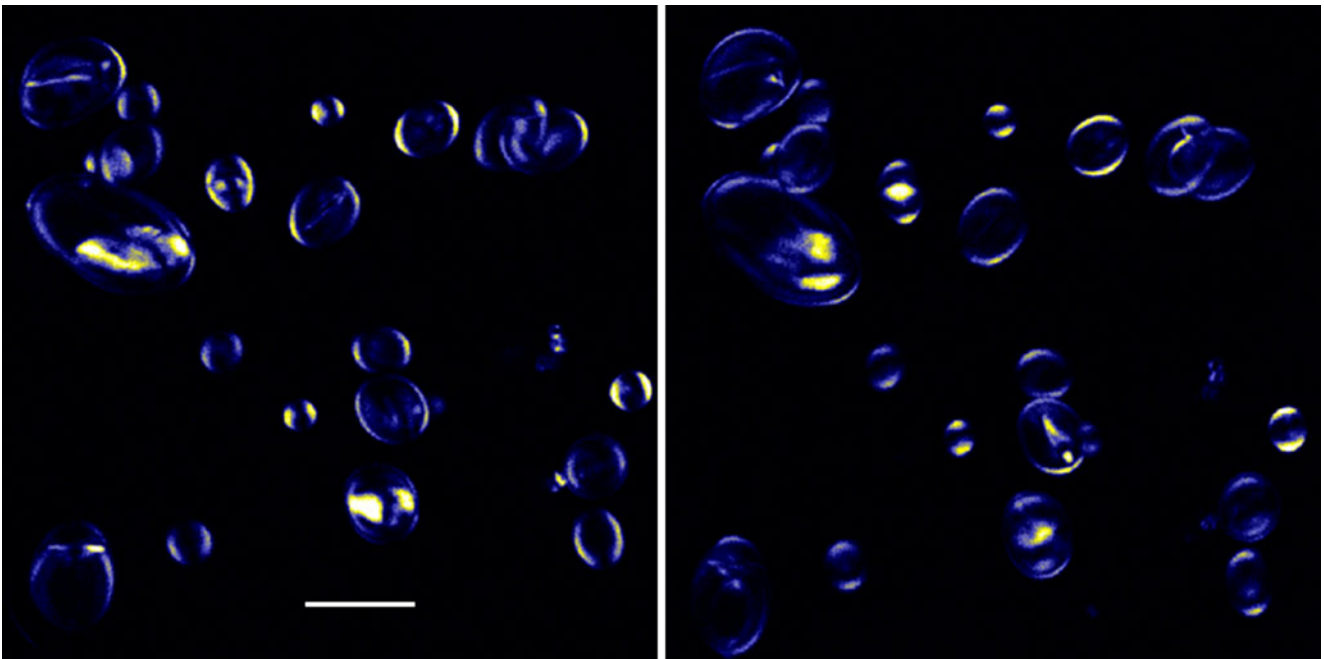


Fig. 9 Isolated starch grains, imaged with two orthogonal directions of polarization of the laser beam. The polarization dependence of the SH signal is evident. Scale bar 50 μm . See Cox et al. (2005)

Fig. 10 Zones of recrystallization (*green*, SHG) in stored rice-flour paste. *Red* and *blue* channels are autofluorescence. Sample courtesy of Les Copeland and Chiming Tan. *Scale bar* 25 μm . See Cox et al. (2005)

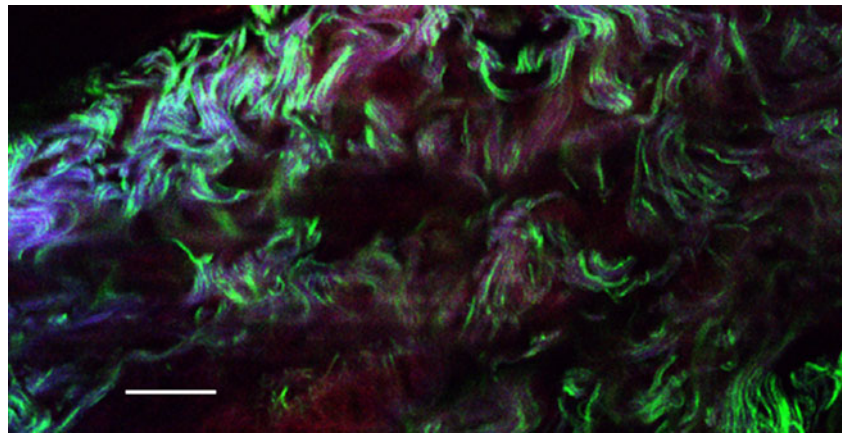
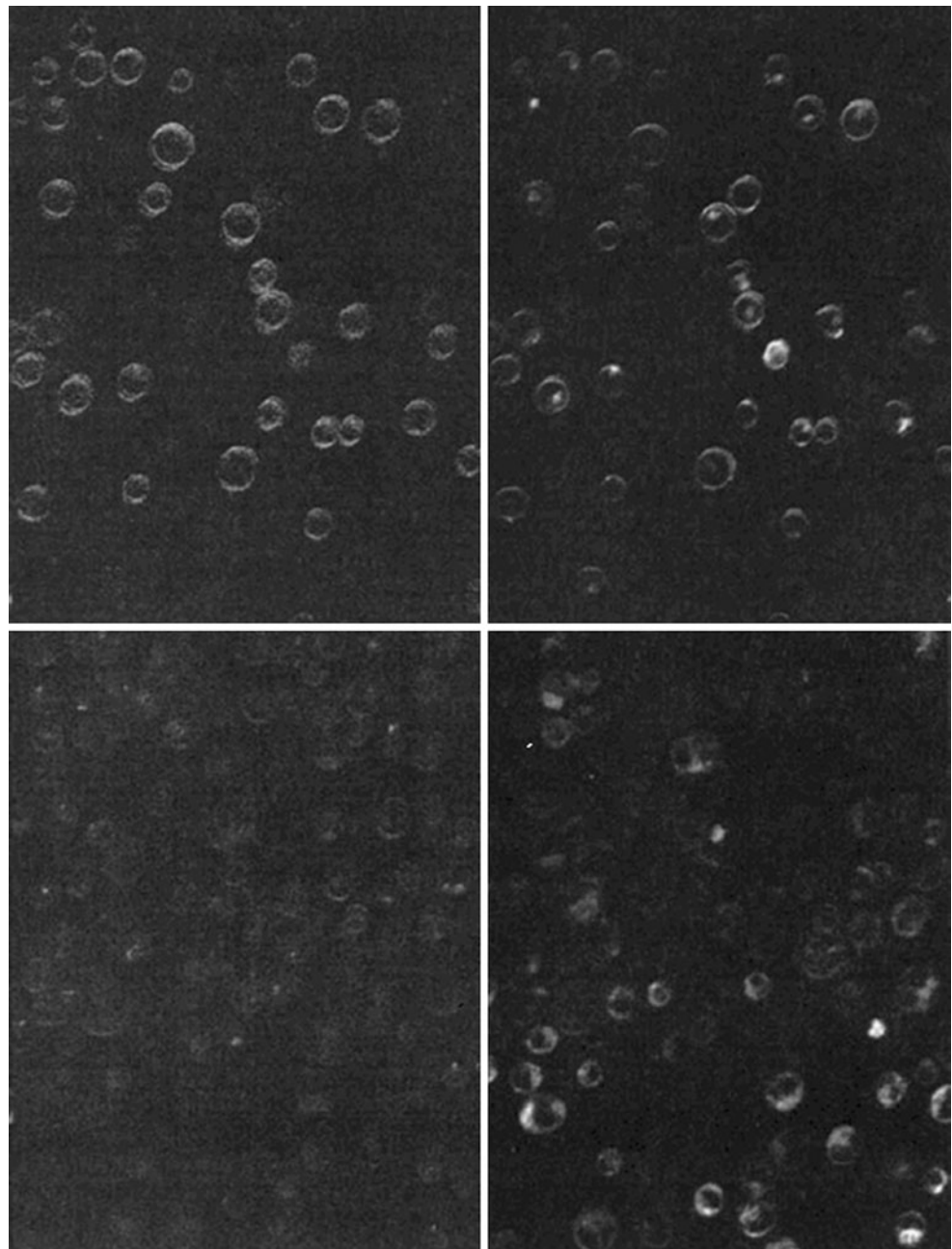


Fig. 11 The membrane potential dye ANEP labelling the membrane of L1210 lymphocytes. *Upper* low potassium concentration, *lower* high potassium. *Left* SHG signal, *right* fluorescence. From Campagnola et al. (2001), by permission of Journal of Biomedical Optics



improve product texture is a key goal of food technology. Since the strength of the SH signal is strongly dependent on crystallinity, SHG microscopy promises to be a very effective tool for imaging this process. Figure 10 shows an example: a rice-starch and water paste which has been stored and begun to crystallise. Zones of crystallization give a strong SH signal.

Potentiometric SHG dyes

Most SHG microscopy to date has made use of intrinsic harmonic generation properties of cell components. However, there is no reason we cannot use compounds which will generate the second harmonic as labels. This has been applied to fast-responding probes which measure membrane potential. If a molecule has an excited electron state at the same energy level as the second harmonic, it will enhance the SH signal: resonance enhanced SHG. This has been made use of with styryl potential-sensitive dyes, which are strongly and directionally affected by electric fields, and therefore give both SHG and TPF signals. These dyes are much faster-responding than other potential indicating dyes, but show a very weak change in fluorescence, so the second harmonic signal can be much more

useful. This technique was first pioneered in Leslie Loew's laboratory (Campagnola et al. 2001).

Figure 11 shows a demonstration of the dye ANEP indicating potential in lymphocytes, and shows clearly that the change in SH signal (left images) is more marked than the change in fluorescence (right images). Pons et al. (2003) investigated, using giant vesicles, the factors determining the performance of these dyes. They showed that two different factors are involved, an electro-optic-induced alteration in the molecular hyperpolarizability (that is the ability to generate the second harmonic) and secondly an electric-field induced alteration of the degree of molecular alignment. Clearly for an optimized dye these must work together, but in the early dyes they tended to work in opposition. They evaluated the relative weights of these contributions and made initial attempts at finding an optimal dye. They also calculated from basic principles the possible response times of these dyes, and showed that it would be sub-millisecond.

Not surprisingly, given the potential for high sensing speed, the major application since then has been in neurobiology. Several laboratories have sought to exploit the properties of these dyes to measure signal transmittal in neurons (Dombeck et al. 2005; Nuriya et al. 2006). The dye of choice has been FM4-64. Because of the spatial constraints required for SH generation, only dye which is

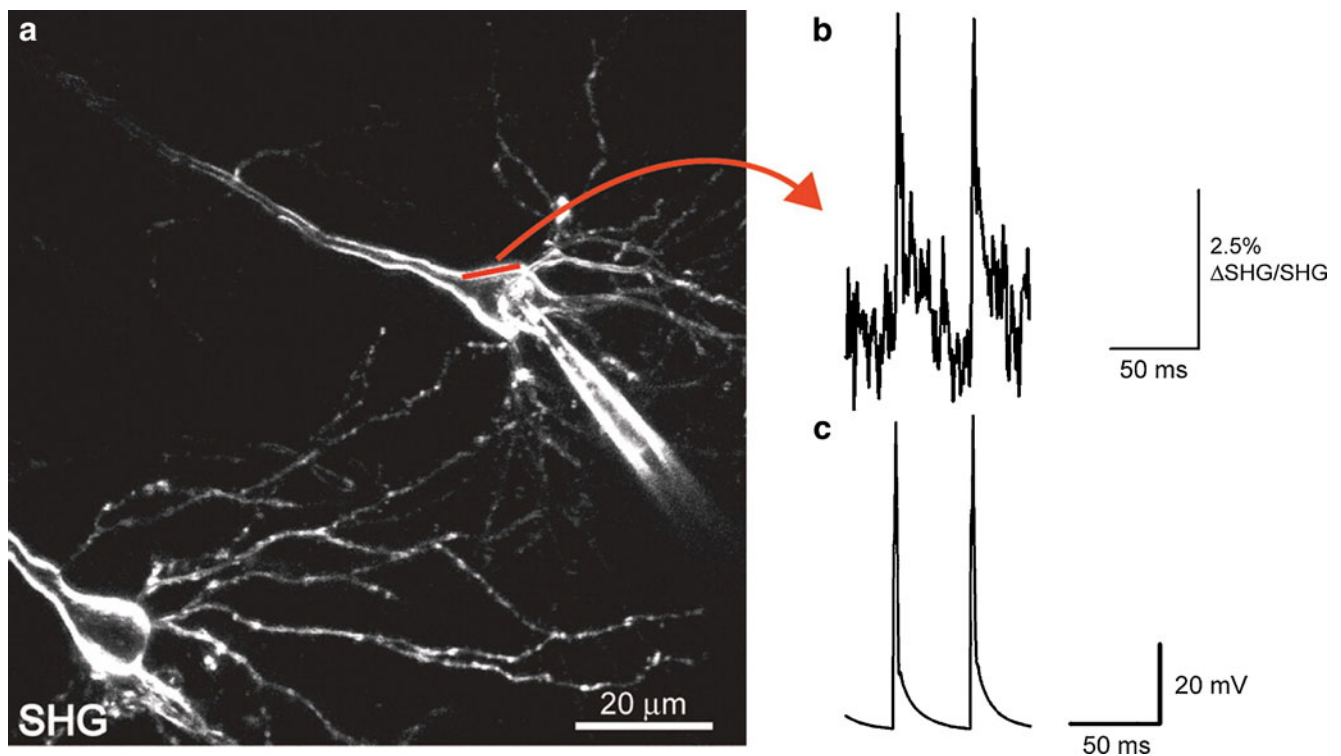


Fig. 12 Fast SHG line scan recording of elicited action potentials in brain slice. **a** This neuron was patch clamped and filled with FM4-64. Straight red line represents scanned line where elicited APs were recorded optically by integrating over the width. **b** SHG recording

intensity versus time from 55 averaged scans (1,200 lines/s) of the line shown in (a). **c** Average current-clamp trace of elicited APs recorded optically in (b). From Dombeck et al., *J. Neurophysiol.* 2005, Am Physiol Soc, used with permission

attached to the membrane gives a signal, which means that the signal to noise ratio is hugely improved relative to fluorescent probes (Dombeck et al. 2005). Figure 12 shows the results which can be achieved. Clearly, the optical and temporal resolution is adequate to measure potential changes over single figure millisecond time periods.

Nuriya et al. (2006) used the properties of SHG dyes to investigate the role of dendritic spines, in particular whether they are actively involved in signal transduction or merely storage compartments. They showed that action potentials did in fact enter the spines. More recently, Jiang and Yuste (2008) have set out to optimize the technology using photon counting since the limiting factor in all these experiments is signal to noise ratio, and therefore further advances are contingent on improving it.

Conclusions

Second harmonic microscopy has a strange, Cinderella-like history. It was first demonstrated 16 years before two-photon microscopy, yet multiphoton fluorescence became a mainstream technique immediately after the first demonstration, while second harmonic microscopy only came into general use 10 years later. It is now widely used for collagen imaging—to the point where at least two commercial dedicated systems are on the market—and becoming known for imaging myosin and starch. The originally slightly obscure idea of SHG potentiometric dyes has found a major niche in neurobiology and seems destined to grow. What took you so long?

References

- Brüggemann DA, Brewer J, Risbo J, Bagatolli L (2010) Second harmonic generation microscopy: A tool for spatially and temporally resolved studies of heat induced structural changes in meat. *Food Biophysics* 5:1–8
- Campagnola PJ, Clark HA, Mohler WA, Lewis A, Loew LM (2001) Second harmonic imaging microscopy of living cells. *J Biomed Opt* 6:277–286
- Campagnola PJ, Millard AC, Terasaki M, Hoppe PE, Malone CJ, Mohler WA (2002) Three-dimensional high-resolution second-harmonic generation imaging of endogenous structural proteins in biological tissues. *Biophys J* 81:493–508
- Chen M-H, Chen WL, Sun Y, Fwu PT, Dong C-Y (2007) Multiphoton autofluorescence and second-harmonic generation imaging of the tooth. *J Biomed Opt* 12:064018
- Chu S-W, Chen I-H, Liu T-M, Chen PC, Sun CK (2001) Multimodal nonlinear spectral microscopy based on a femtosecond Cr:forsterite laser. *Opt Lett* 26:1909–1911
- Cox GC, Manconi F, Kable EPK (2002) Second harmonic imaging of collagen in mammalian tissue. *Proc SPIE* 4620:148–156
- Cox GC, Kable E, Jones A, Fraser I, Manconi F, Gorrell M (2003) 3-dimensional imaging of collagen using second harmonic generation. *J Struct Biol* 141:53–62
- Cox GC, Kable EP (2006) Second harmonic imaging of collagen. In: Taatjes DJ, Mossman BT (eds) *Cell imaging techniques. Methods in molecular biology*, vol 319. Humana Press, Totowa, NJ, pp 15–35
- Cox GC, Moreno N, Feijó JM (2005) Second-harmonic imaging of plant polysaccharides. *J Biomed Opt* 10:024013
- Denk W, Strickler JH, Webb WW (1990) Two photon laser scanning fluorescence microscopy. *Science* 248:73–76
- Dombeck DA, Sacconi L, Blanchard-Desce M, Webb WW (2005) Optical recording of fast neuronal membrane potential transients in acute mammalian brain slices by second-harmonic generation microscopy. *J Neurophysiol* 94:3628–3636
- Franken PA, Hill AE, Peters CW, Weinreich G (1961) Generation of optical harmonics. *Phys Rev Lett* 7:118–119
- Freund I, Deutsch M, Sprecher A (1986) Connective tissue polarity. Optical second-harmonic microscopy, crossed-beam summation, and small-angle scattering in rat-tail tendon. *Biophys J* 50:693–712
- Fung DT, Sereysky JB, Basta-Pljakic J, Laudier DM, Huq R, Jepsen KJ, Schaffler MB, Flatow EL (2010) Second harmonic generation imaging and Fourier transform spectral analysis reveal damage in fatigue-loaded tendons. *Ann Biomed Eng* 38:1741–1751
- Gailhouste L, Le Grand Y, Odin C, Guyader D, Turlin B, Ezan F, Désille Y, Guilbert T, Bessard A, Frémin C, Theret N, Baffet G (2010) Fibrillar collagen scoring by second harmonic microscopy: a new tool in the assessment of liver fibrosis. *J Hepatol* 52:398–406
- Gannaway JN, Sheppard CJR (1978) Second harmonic imaging in the scanning optical microscope. *Opt Quantum Electro* 10:435–439
- Georgiou E, Theodossiou T, Hovhannisyva V, Politopoulos K, Rapti GS, Yova D (2000) Second and third optical harmonic generation in type I collagen, by nanosecond laser irradiation, over a broad spectral region. *Opt Commun* 176:253–260
- Gorrell MD, Wang XM, Levy MT, Kable E, Marinos G, Cox G, McCaughan GW (2003) Intrahepatic expression of collagen and fibroblast activation protein (FAP) in hepatitis C virus infection. *Adv Exp Med Biol* 524:235–243
- Hellwarth R, Christensen P (1974) Nonlinear microscopic examination of structure in polycrystalline ZnSe. *Opt Commun* 12:318–322
- Jiang J, Yuste R (2008) Second-harmonic generation imaging of membrane potential with photon counting. *Microsc Microanal* 14:526–531
- König K, Riemann I (2003) High-resolution multiphoton tomography of human skin with subcellular spatial resolution and picosecond time resolution. *J Biomed Opt* 8:432–439
- Lodish H, Berk A, Lipursky SL, Matsudaira P, Baltimore D, Darrell J (2000) *Molecular cell biology*, 4th edn. Freeman, New York
- Manconi F, Kable EP, Cox GC, Markham R, Fraser IS (2003) Whole-mount sections displaying microvascular and glandular structures in human uterus using multiphoton excitation microscopy. *Micron* 34:351–358
- Mizutani G, Sonoda Y, Sano H, Sakamoto M, Takahashi T, Ushioda S (2000) Detection of starch granules in a living plant by optical second harmonic microscopy. *J Lumin* 87:824–826
- Mohler W, Millard AC, Campagnola PJ (2003) Second harmonic generation imaging of endogenous structural proteins. *Methods* 29:97–109
- Moreno N, Feijo J, Cox G (2004) Implementation and evaluation of a detector for forward propagated second harmonic signals. *Micron* 35:721–724
- Nadiarnykh O, Lacombe RB, Brewer MA, Campagnola PJ, et al (2010) Alterations of the extracellular matrix in ovarian cancer studied by Second Harmonic Generation imaging microscopy. *BMC Cancer* 10:94–142
- Nucciotti V, Stringari C, Sacconi L, Vanzì F, Fusi L, Linari M, Piazzesi G, Lombardi V, Pavone FS (2010) Probing myosin structural

- conformation in vivo by second-harmonic generation microscopy. *Proc Natl Acad Sci USA* 107:7763–7768
- Nuriya M, Jiang J, Nemet B, Eisenthal KB, Yuste R (2006) Imaging membrane potential in dendritic spines. *Proc Nat Acad Sci USA* 103:786–790
- Pons T, Moreaux L, Mongin O, Blanchard-Desce M, Mertz J (2003) Mechanisms of membrane potential sensing with second-harmonic generation microscopy. *J Biomed Opt* 8:428–431
- Provenzano PP, Eliceiri KW, Yan L, Ada-Nguema A, Conklin MW, Inman DR, Keely PJ (2008) Nonlinear optical imaging of cellular processes in breast cancer. *Microsc Microanal* 14:532–548
- Raja AM, Xu S, Zhou J, Tai DCS, Chen CS, Yu H (2010) Pulse-modulated second harmonic imaging microscope imaging quantitatively demonstrates marked increase of collagen in tumor after chemotherapy. *J Biomed Opt* 15:056016
- Ralston E, Swaim B, Czapiga M, Hwud W-L, Chien Y-H, Pittis MG, Bembi B, Schwartz O, Plotz P, Raben N (2008) Detection and imaging of non-contractile inclusions and sarcomeric anomalies in skeletal muscle by second harmonic generation combined with two-photon excited fluorescence. *J Struct Biol* 162:500–508
- Roth S, Freund I (1981) Optical second-harmonic scattering in rat-tail tendon. *Biopolymers* 20:1271–1290
- Sivaguru M, Durgam S, Ambekar R, Luedtke D, Fried G, Stewart A, Toussaint KC (2010) Quantitative analysis of collagen fiber organization in injured tendons using Fourier transform-second harmonic generation imaging. *Opt Express* 18:24983–24993
- Tai DC, Tan N, Xu S, Kang CH, Chia SM, Cheng CL, Wee A, Wei CL, Raja AM, Xiao G, Chang S, Rajapakse JC, So PT, Tang HH, Chen CS, Yu H (2009) Fibro-C-Index: comprehensive, morphology-based quantification of liver fibrosis using second harmonic generation and two-photon microscopy. *J Biomed Opt* 14(044013):1–10
- Wallace SJ, Morrison JL, Botting KJ, Kee TW (2008) Second-harmonic generation and two-photon-excited autofluorescence microscopy of cardiomyocytes: quantification of cell volume and myosin filaments. *J Biomed Opt* 13:064018
- Williams RM, Zipfel WR, Webb WW (2004) Interpreting second harmonic generation images of collagen I fibrils. *Biophys J* 88:1377–1386
- Xu P, Cox G, Ramshaw JAM, Lukins P and Sheppard CJR (2004) Polarization effects in SHG of collagen. *Proceedings of SPIE* 5323, 343–352
- Xu P, Kable EP, Sheppard CJR, Cox G (2010) A quasi-crystal model of collagen microstructure based on SHG microscopy. *Chin Opt Lett* 8:213–216
- Zipfel WR, Williams RM, Christie R, Nitikin AY, Hyman BT, Webb WW (2003) Live tissue intrinsic emission microscopy using multiphoton excited native fluorescence and second harmonic generation. *Proc Nat Acad Sci USA* 100:7075–7080
- Zhou R, Lu H, Liu X, Gong Y, Mao D (2010) Second-harmonic generation from a periodic array of noncentrosymmetric nanoholes. *J Opt Soc Am B* 27:2405–2409